Modeling of gate bias modulation in carbon nanotube field-effect transistor

Toshishige Yamada[a)]

NASA Ames Research Center, M/S 229-1, Moffett Field, California, 94035-1000

(Received)

The threshold voltages of a carbon-nanotube (CNT) field-effect transistor (FET) are studied. The CNT channel is so thin that there is no voltage drop perpendicular to the gate electrode plane, and this makes the device characteristics quite unique. The relation between the voltage and the electrochemical potentials, and the mass action law for electrons and holes are examined in the context of CNTs, and inversion and accumulation threshold voltages (V_{Ti} and V_{Ta}) are derived. V_{Ti} of the CNTFETs has a much stronger doping dependence than that of the metal-oxide-semiconductor FETs, while V_{Ta} of both devices depends weakly on doping with the same functional form.

Recently, there have been a lot of experiments on carbon nanotube (CNT) field-effect transistors (FET) [1,2]. One of the important quantities to characterize the FET operation is a threshold voltage V_T [3]. When the gate voltage V_G exceeds V_T, the FET channel appears and the transistor turns on. In the usual metal-oxide-semiconductor (MOS) FETs, there is an appreciable potential drop in the semiconductor substrate perpendicular to the gate electrode plane, so that the applied V_G will be shared with the gate oxide region and the semiconductor region. The standard V_T expression for the MOSFETs reflects this physics [3]. However, this is not the case in the CNTFETs. A voltage drop in the same perpendicular (diameter) direction is not possible due to the extremely thin CNT, and this will influence the device properties. In this article, we will study the energy band diagrams for the CNTFET by reconsidering the relation between the voltage and the electrochemical potentials, and the mass action law for electrons and holes in the CNT. Then, we will express V_T for the CNTFET, which will show a significantly different doping dependence from that of the MOSFET.

Figure 1 shows the band diagrams for a p-doped MOSFET and a p-doped CNTFET with a metallic gate electrode: (a) MOSFET hole accumulation, (b) MOSFET electron inversion, (c) CNTFET hole accumulation, and (d) CNTFET electron inversion. In the metal side, Φ_m' is a work function subtracted by the oxide electron affinity χ_{ox} and μ_m is an electrochemical potential (Fermi level). In the semiconductor side, Φ_s' is a CNT work function subtracted by χ_{ox}. E_c and E_v are conduction and valence band edges, and E_i is an intrinsic level. μ_s is an electrochemical potential (grounded), and the chemical potential μ_s - E_v is independent of V_G deep inside the substrate. The application of V_G causes the voltage drop in the oxide V_{ox} and the formation of a surface potential Ψ_s. All these quantities are given in the same unit (e.g. volt). In the MOSFET, μ_m

$-\mu_s = V_G$ holds as usual [4]. Regardless of accumulation ($V_G < 0$) in Fig. 1(a) or inversion ($V_G > 0$) in Fig. 1(b), we have

$$\Phi_m' - V_G = V_{ox} + \Phi_s' - \Psi_s \ . \tag{1}$$

However, such Ψ_s is not possible in the CNTFET. In fact, in a bulk semiconductor, the Debye length, a characteristic length for the potential change [3], is at least 100 Å for the dielectric constant $\varepsilon_r \sim 10^1$ and the impurity density $N_{imp} < \sim 10^{18}$ cm^{-3}, but this is still an order of magnitude larger than the CNT diameter. Another way to say this is that an electron wave can maintain its coherency in the CNT diameter direction and subbands are formed so that there will be no potential drop in that direction. V_G attracts opposite charges from the source/drain electrodes to the CNT channel, and the entire CNT is charged. Thus, μ_s will shift from its intrinsic value μ_{s0} and the chemical potential $\mu_s - E_v$, which does not change inside the substrate of the MOSFET, will also change.

We will see the relation $\mu_m - \mu_s = V_G$ [4] still holds in the CNTFET. Because there are a macroscopic number of states in the CNT [5], the usual entropy (S) maximum condition prevails in equilibrium [6]. This is true when the Coulomb charging energy of e^2/C_{NT} is negligible [7], where C_{NT} is a CNT capacitance [2] and e is a unit charge. We let reservoir m at voltage V_m and reservoir s at voltage V_s interact (via a battery of $V_m - V_s$), while keeping the total energy $U = U_m + U_s$, the total charge $Q = Q_m + Q_s$, and the total carriers $N = N_m + N_s$ to be constant, respectively (i.e., $\delta U = \delta U_m + \delta U_s = 0$, etc.). Using the perfect differential $dS = dU/T + VdQ/T - e\mu dN/T$ where T is the temperature and μ is given in the units of volt, we have $\delta(S_m + S_s) = (1/T_m - 1/T_s)\delta U_s + (V_m/T_m - V_s/T_s)\delta Q_s - e(\mu_m/T_m - \mu_s/T_s)\delta N_s$ for the unified system. Because $\delta S = 0$ in equilibrium, each coefficient must vanish. The charge and the carriers are related by $Q = eN$. Thus, we have $T_m = T_s$ and $V_m - V_s = \mu_m - \mu_s$. Therefore, the band diagrams in Fig. 1(c) and 1(d)

are established, where $\Delta\mu_s = \mu_s - \mu_{s0}$. Regardless of accumulation ($V_G < 0$) in Fig. 1(c) or inversion ($V_G > 0$) in Fig. 1(d), we have

$$\Phi_m' - V_G = V_{ox} + \Phi_s' - \Delta\mu_s \ . \tag{2}$$

As in the bulk p-semiconductors [4], we can express the hole density $p = N_a \exp(-\beta\Delta\mu_s) = n_i \exp[\beta(E_i-\mu_s)]$ and the electron density $n = (n_i^2/N_a) \exp(\beta\Delta\mu_s) = n_i \exp[\beta(\mu_s-E_i)]$ in the p-CNT, where n_i is an intrinsic carrier density, N_a is an acceptor density, and $\beta = e/k_BT$ with k_B the Boltzmann constant. The unique one-dimensional band properties are all embedded in the band gap $E_g = E_c - E_v$ and in n_i. We then notice $pn = n_i^2$ regardless of μ_s in the CNT, or the mass action law prevails. This is justified as follows. When electron-hole pairs are generated thermally (the process independent of impurities), the same number of electron-hole pairs must be annihilated in equilibrium. The annihilation rate is proportional to the electron-hole collision probability, or the pn product, and should be independent of μ_s to compensate the thermal generation. This argument uses none of the details of the hardware [8], and it is not surprising that n and p are given as above.

We will express V_G as a function of $\Delta\mu_s$ in the CNTFET. From Eq. (2), we have $V_G - V_{FB} = \Delta\mu_s - V_{ox} = \Delta\mu_s + e(n+N_a-p)/C_{NT} = \Delta\mu_s + e[(n_i^2/N_a)\exp(\beta\Delta\mu_s)+N_a-N_a\exp(-\beta\Delta\mu_s)]/C_{NT}$, where $V_{FB} = \Phi_m' - \Phi_s'$ is a flat band voltage. The linear term of charge contributes to V_G due to the *absence* of the field in the charged region, reminiscent of a parallel capacitor. The corresponding relation between V_G and Ψ_s in the MOSFET is $V_G - V_{FB} = \pm\Psi_s \pm(2\varepsilon k_BTN_a)^{1/2}\{\exp(-\beta\Psi_s)+\beta\Psi_s-1 + (n_i/N_a)^2[\exp(\beta\Psi_s)-\beta\Psi_s-1)]\}^{1/2}/C_{ox}$ (the same sign as Ψ_s), where C_{ox} is an oxide capacitance and ε is a permittivity [3]. The square root term of charge contributes to V_G due to the *presence* of the field this time, reminiscent of a pn-junction [4]. Figure 2 shows $|V_G - V_{FB}|$ as a function of $\Delta\mu_s$ in the CNTFET or Ψ_s in the MOSFET. For the former, $N_a = 10^6$ and 3×10^6 cm^{-1} with $C_{NT} =$

0.237 pF/cm [9], and for the latter, $N_a = 10^{16}$ cm^{-3} and the oxide thickness $d_{ox} = 100$ Å [10] are chosen. $\Psi_F = (k_BT/e)ln(N_a/n_i)$ is a Fermi level measured from E_i. $\Delta\mu_s$ or $\Psi_s = 0$ corresponds to the flat band condition, and $\Delta\mu_s$ or $\Psi_s = 2\Psi_F$ corresponds to the onset of strong inversion. Once they occur, $dV_G/d\Delta\mu_s$ and $dV_G/d\Psi_s$ are quite large in both devices. This means that once the transistor channel appears, the channel electrons or holes can screen V_G effectively so that $\Delta\mu_s$ or Ψ_s will not change significantly. The screening is different in both devices, such that the CNTFET behaves as $V_G \sim \exp(\beta|\Delta\mu_s|)$ while the MOSFET behaves as $V_G \sim \exp(\beta|\Psi_s|/2)$.

This difference leads to different threshold behaviors. Writing a doping independent part of V_{FB} by $V_0 = \Phi_m' - \chi_{ox} - E_G/2$, we have $V_{FB} = V_0 \pm \Psi_F$, where - is chosen for p-type with N_a and + is chosen for n-type with the donor density N_d. For an originally p-doped device, we have an accumulation threshold V_{Ta} for the p-channel formation, and an inversion threshold V_{Ti} for the n-channel formation. We here derive both V_{Ta} and V_{Ti}, following the recent CNTFET experiments [1,2]. With a dimensionless Fermi level $X = e\Psi_F/k_BT = ln(N_{imp}/n_i)$, we have:

(a) accumulated p-channel formation threshold (originally p-doped)

$$V_{Ta} = V_0 - k_BTX/e \ , \qquad \text{(CNTFET, MOSFET)} \qquad (3)$$

(b) inverted n-channel formation threshold (originally p-doped)

$$V_{Ti} = V_0 + k_BTX/e + 2en_i\exp(X)/C_{NT} \ , \qquad \text{(CNTFET)} \qquad (4)$$

$$V_{Ti} = V_0 + k_BTX/e + 2(\varepsilon k_BTn_i)^{1/2}X^{1/2}\exp(X/2)/C_{ox} \ , \qquad \text{(MOSFET)} \qquad (5)$$

(c) accumulated n-channel formation threshold (originally n-doped)

$$V_{Ta} = V_0 + k_BTX/e \ , \qquad \text{(CNTFET, MOSFET)} \qquad (6)$$

(d) inverted p-channel formation threshold (originally n-doped)

$$V_{Ti} = V_0 - k_BTX/e - 2en_i\exp(X)/C_{NT} \ , \qquad \text{(CNTFET)} \qquad (7)$$

$$V_{Ti} = V_0 - k_BTX/e - 2(\varepsilon k_BTn_i)^{1/2}X^{1/2}\exp(X/2)/C_{ox} \ , \qquad \text{(MOSFET)} \qquad (8)$$

where n_i, N_{imp}, and V_0 have to be evaluated for CNTFET and MOSFET separately. V_{Ta} does not depend on doping very much and is linear in X. This simply reflects the doping dependence of V_{FB} though Φ_s'. V_{Ti} depends drastically on doping, and the CNTFET has a much stronger dependence ~exp(X) than the MOSFET ~$X^{1/2}$exp($X/2$).

Figure 3 shows V_{Ti} and V_{Ta} for electrons and holes as a function of X in the CNTFET and the MOSFET. V_T's in the CNTFET are drawn for $n_i/C_{NT} = 10^{14}$ F^{-1} and 10^{12} F^{-1} with $V_0 = 1$ V [11], where V_{Ti} starts diverting from V_0 significantly at about $X \sim ln(C_{NT}|V_0|/2en_i)$. For comparison, V_T's in the MOSFET are drawn for $d_{ox} = 100$ Å and $V_0 = -0.5$ V [10] with corresponding N_{imp} at the top horizontal ticks. V_{Ti} changes more rapidly in the CNTFET than in the MOSFET. V_{Ta} depends quite slowly on X, and has the same functional dependence in both devices. In the CNTFET, V_{Ti} for the p-channel device with $V_0 > 0$ will change its sign as N_d increases, while in the MOSFET, V_{Ti} for the n-channel device with $V_0 < 0$ will change its sign as N_a increases. The sign change in V_T indicates transitions from normally-on device to normally-off device, and this has to be aware in the circuit design [3,10]. Which channel device will go through the transition is related to the sign of V_0, i.e., the gate material and the trapped/interface charges [3].

In this article, we have assumed that the source/drain contacts are Ohmic (ideal) for both electrons and holes. Currently, achieving Ohmic contact for electrons is not trivial [1,2,12], but this technology is mandatory in every electronics. We have also assumed the metallic gate electrode allowing no voltage drop. These are consistent with the future direction of CNT electronics.

We have shown that the doping dependence of V_{Ti} in the CNTFET is strong and is significantly different from that in the MOSFET, while that of V_{Ta} is weak and has the same functional form. This is because there is no potential drop in the diameter direction of a CNT channel.

The author gratefully acknowledges discussions with T. R. Govindan and M. Meyyappan.

Figure captions

FIG. 1 Band diagrams for a p-doped MOSFET and a p-doped CNTFET with schematic charge distributions: (a) MOSFET hole accumulation, (b) MOSFET electron inversion, (c) CNTFET hole accumulation and (d) CNTFET electron inversion, where narrow CNT diagrams are widened for clarity. Φ_m' and Φ_s' are work functions minus the oxide electron affinity. μ_m and μ_s (grounded) are electrochemical potentials. V_G is a gate voltage and V_{ox} is a potential drop. E_c and E_v are band edges, and E_i is an intrinsic level. Ψ_s is a surface potential and $\Delta\mu_s = \mu_s - \mu_{s0}$, where μ_{s0} is an initial μ_s. All quantities are given in the same energy unit.

FIG. 2 $|V_G - V_{FB}|$ as a function of either $\Delta\mu_s$ or Ψ_s. Two plots with $N_a = 10^6$ and 3×10^6 cm^{-1} for the CNTFET are shown and are compared to those for the MOSFET with $N_a = 10^{16}$ cm^{-3}. The locations of the band edges E_c and E_v, and the intrinsic level E_i are indicated. The flat band (FB) is achieved at $\Delta\mu_s$ or $\Psi_s = 0$ and the strong inversion starts at $\Delta\mu_s$ or $\Psi_s = 2\Psi_F$. $\Delta\mu_s$ or $\Psi_s < 0$ corresponds to accumulation.

FIG. 3 Threshold voltages V_T's as a function of dimensionless doping density X. V_{Ti}'s for electron- and hole-inversions (e-inv and h-inv) in the CNTFET with a doping-independent voltage $V_0 = 1$ V are plotted for a parameter $n_i/C_{NT} = 10^{14}$ F^{-1} or 10^{12} F^{-1}, respectively, along with n_i/C_{NT}-independent V_{Ta}'s for electron- and hole-accumulations (e-acc and h-acc). For comparison, V_T's in the MOSFET with an oxide thickness $d_{ox} = 100$ Å and $V_0 = -0.5$ V are plotted, where the upper horizontal ticks show N_{imp} for corresponding X.

References

a) CSC, Electronic mail: yamada@nas.nasa.gov

[1] S. J. Tans, A. R. M. Vershueren, and C. Dekker, Nature (London) **393**, 49 (1998); C. Zhou, J. Kong, and H. Dai, Appl. Phys. Lett. **76**, 1597 (2000); V. Derycke, R. Martel, J. Appenzeller, and Ph. Avouris, Nano Letters **1**, 453 (2001); X. Liu, C. Lee, C. Zhou, and J. Han, Appl. Phys. Lett. **79**, 3329 (2001); A. Bachtold, P. Hadley, T. Nakanishi, and C. Dekker, Science **294**, 1317 (2001).

[2] R. Martel, T. Schmidt, H. R. Shea, T. Hertel, and Ph. Avouris, Appl. Phys. Lett. **73**, 2447 (1998).

[3] S. M. Sze, *Physics of Semiconductor Devices,* 2nd ed. (Wiley, New York, 1981).

[4] W. Shockley, *Electrons and Holes in Semiconductors* (Van Nostrand, Princeton, 1950).

[5] If the number of states is microscopic with discrete energy levels, e.g., quantum dots, the relation will have to be reconsidered as in C. W. J. Beenakker, Phys. Rev. B **44**, 1646 (1991).

[6] R. Kubo, H. Ichimura, T. Usui, and N. Hashitsume, *Statistical Mechanics* (North-Holland, New York, 1965).

[7] D. V. Averin and K. K. Likharev, *Mesoscopic Phenomena in Solids*, edited by B. L. Altshuler, P. A. Lee, and R. A. Webb (Elsevier, Amsterdam, 1991).

[8] E. Fermi, *Thermodynamics* (Dover, New York, 1956).

[9] Due to the cylindrical shape, C_{NT} depends on d_{ox} only logarithmically, and N_a is expected to be on the same order as p in the accumulation. The parameters in Fig. 2 are consistent with C_{NT} = 0.237 pF/cm and $p = 10^6$ cm^{-1} with a band gap of 0.45 eV (radius 0.8 nm) in Ref. 2.

[10] B. G. Streetman and S. Banerjee, *Solid State Electronic Devices*, 5th ed. (Prentice, Englewood Cliffs, 2000).

[11] We estimate $n_i = 10\ \mathrm{cm}^{-1}$ from $p = 10^6\ \mathrm{cm}^{-1}$ in the accumulation in Ref. 2. Using $C_{NT} =$ 0.237 pF/cm in Ref. 2, we have $n_i/C_{NT} \sim 4 \times 10^{12}\ \mathrm{F}^{-1}$. Many CNTFETs are expected to fall into the range of $n_i/C_{NT} \sim 10^{12\text{-}14}\ \mathrm{F}^{-1}$ in Fig. 3.

[12] R. Martel, V. Derycke, C. Lavoie, J. Appenzeller, K. K. Chan, J. Tersoff, and Ph. Avouris, Phys. Rev. Lett. **87**, 256805-1 (2001).

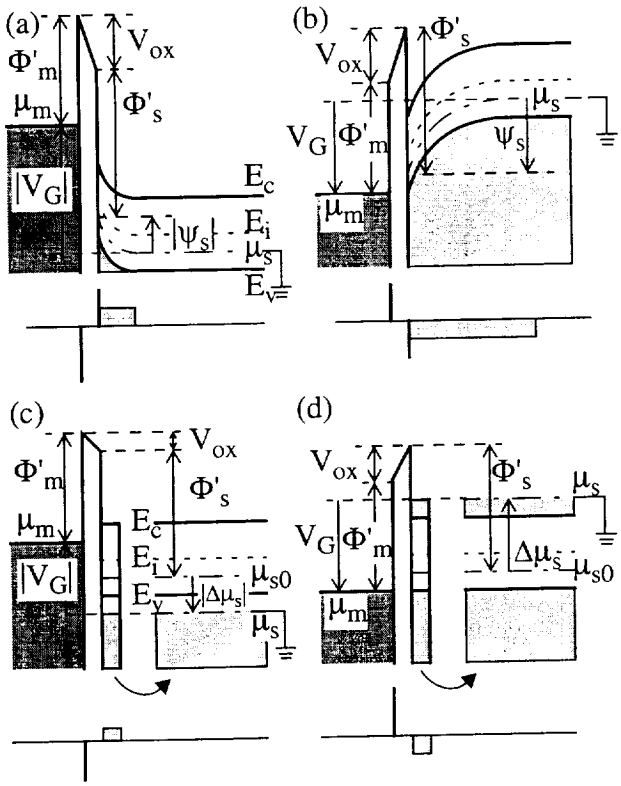

Fig. 1
APL, Yamada

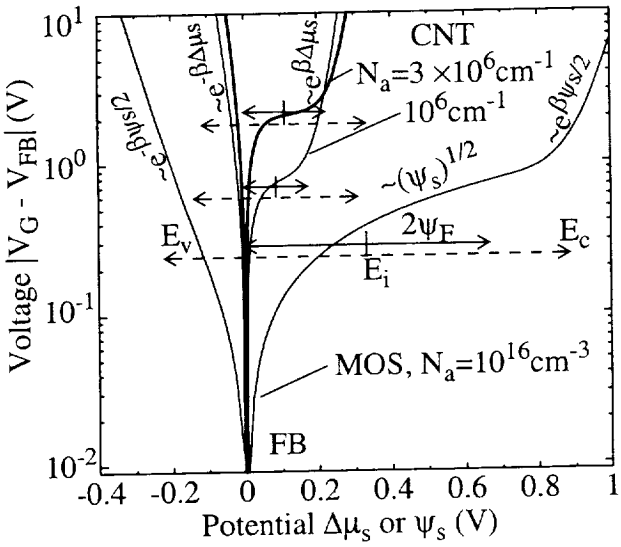

Fig. 2
APL, Yamada

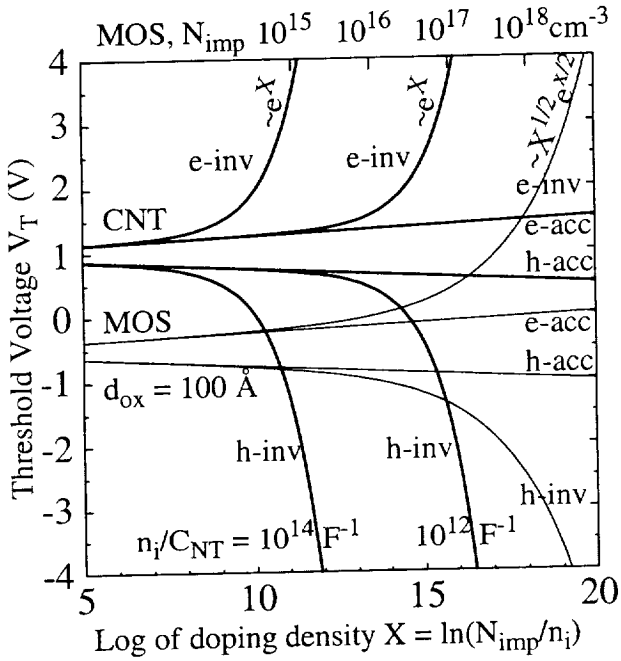

Fig. 3
APL, Yamada